

# A Detailed Quantitative Analysis of B1 Components at 1.5T and 3T

X. Chen<sup>1</sup>, and M. Steckner<sup>1</sup>

<sup>1</sup>Toshiba Medical Research Institute USA, Inc., Mayfield Village, OH, United States

**INTRODUCTION:** While SAR is crucial for the RF safety control of an MR scan,  $B_{1rms}$  (defined as  $\sqrt{\int_0^t [B_1(t)]^2 dt} / t$ , where  $B_1$  is the total RF magnetic field) [1] serves as a supplemental safety metric. For example,  $B_{1rms}$  is useful for defining the MR conditional labeling of implants [1]. An unloaded quadrature driven (QD) birdcage coil generates nearly perfect  $B_1$  with circular polarization:  $B_1^+$  (the tipping component) is homogeneous and  $B_1^-$  (the component rotating counter to the spin precession) is zero and thus  $|B_1^-| \ll |B_1^+|$  is usually assumed [2]. Loading the coil distorts the  $B_1$  field, causing  $B_1^+$  and  $B_1^-$  components. While only  $B_1^+$  is useful for MRI purposes, both components contribute to RF power deposition ( $|B_1| = \sqrt{|B_1^+|^2 + |B_1^-|^2}$ ). In this work we use FDTD (Finite Difference Time Domain) numerical simulations to demonstrate that  $B_1^-$  should not be ignored in loaded coils at either 1.5T or 3T.

**METHODS:** All simulations were performed with xFDTD and 39 tissue Visible Man model (both from Remcom, Inc., State College, PA) using a 24 rung high pass birdcage coil [3], with 63cm diameter, 68cm shield diameter and 70cm length (both coil and shield). The coil model was tuned to 64MHz (1.5T) and 128MHz (3T) respectively with appropriate end-ring capacitors. QD was generated with two voltage sources of equal amplitude but 90 degree phase difference in one end-ring. The heart was aligned with the coil center, and the back was 13cm below the coil center (Fig.1). Frequency appropriate tissue parameters (dielectric permittivity and conductivity) were used.  $B_1^+$  and  $B_1^-$  components for both unloaded and loaded situations were recorded after all simulations converged to steady state.

**RESULTS:** Fig. 2 shows  $B_1^+$  and  $B_1^-$  maps for unloaded coil model at 1.5T and 3T. At both field strengths,  $|B_1^+|$  is highly uniform and  $|B_1^-|$  is negligible, confirming the  $|B_1^-| \ll |B_1^+|$  assumption. Fig. 3 shows the distortions to  $B_1$  fields due to loading. Numerical evaluations of  $|B_1^-|/|B_1^+|$  at coil center and averaged in central axial slice (Table 1) show that the  $|B_1^-| \ll |B_1^+|$  assumption is violated at 1.5T and more significantly at 3T. As a result, using  $|B_1^+|$  alone will underestimate total  $B_1$  field strength (see  $|B_1^+|/|B_1|$  in Table 1) by up to 16%, on average over a 25 cm radius within the central axial slice and up to 74% within a 1 cm radius at 3T.

**CONCLUSIONS:** Numerical simulations show that loaded coils have distorted circularly polarized  $B_1$  fields at both 1.5T and 3T. Ignoring  $B_1^-$  contributions results in underestimating total  $B_1$  field strength. Total  $B_1$  is essential for estimating implant risk and for the development of in-vivo SAR measurement [2, 4-6]. Additionally,  $B_1^-$  contribution can be more significant in parallel transmit systems than birdcage coils. Modeling and experiments are needed to accurately understand all contributions to total  $B_1$  field for various imaging conditions.

**REFERENCES:** [1] IEC 60601-2-33, 3<sup>rd</sup> edition. [2] T. Voigt et al., ISMRM 2010, p. 3876. [3] W. Liu et al., Appl. Magn. Reson. 29 (2005): pp 5-18. [4] T. Voigt et al., ISMRM 2009, p. 4513. [5] M. A. Cloos et al., ISMRM 2009, p. 3037. [6] U. Katscher et al., ISMRM 2009, p. 4512.

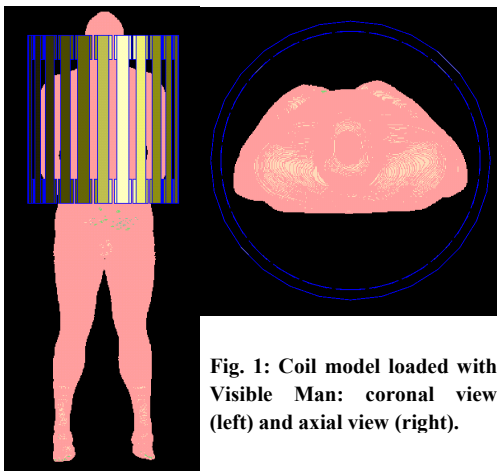


Fig. 1: Coil model loaded with Visible Man: coronal view (left) and axial view (right).

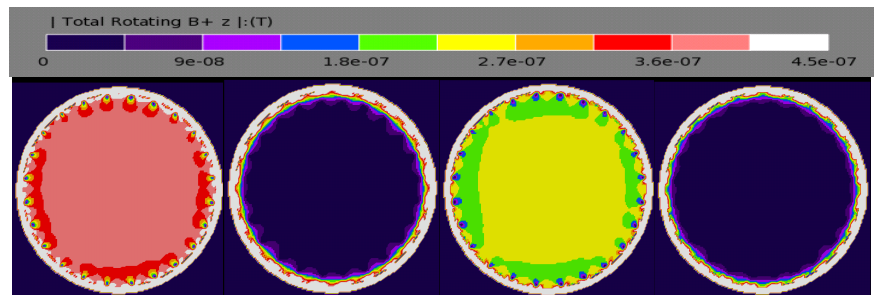


Fig. 2:  $B_1$  maps for unloaded birdcage coil: (from left to right)  $B_1^+$  at 1.5T,  $B_1^-$  at 1.5T,  $B_1^+$  at 3T, and  $B_1^-$  at 3T.

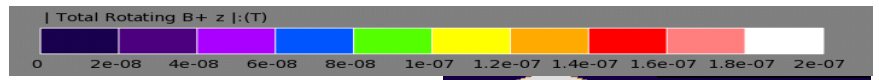


Fig. 3:  $B_1$  maps for loaded birdcage coil:  $B_1^+$  at 1.5T (upper left),  $B_1^-$  at 1.5T (upper right),  $B_1^+$  at 3T (lower left), and  $B_1^-$  at 3T (lower right).

| Unloaded | Main Magnetic Field Strength | $ B_1^- / B_1^+ $ at coil center | $ B_1^- / B_1^+ $ averaged over central axial slice | $ B_1^+ / B_1 $ averaged over central axial slice |
|----------|------------------------------|----------------------------------|---|---|
|          | 1.5T                         |                                  | 2%  | 3%  |
| 3T       |                              | 1%                               | 3%  | 1   |

| Loaded | Main Magnetic Field Strength | $ B_1^- / B_1^+ $ at coil center | $ B_1^- / B_1^+ $ averaged over central axial slice | $ B_1^+ / B_1 $ averaged over central axial slice | Min $ B_1^- / B_1^+ $ averaged over 1cm radius in central axial slice |
|--------|------------------------------|----------------------------------|---|---|---|
|        | 1.5T                         |                                  | 39%   | 44%   | 92%   |
| 3T     |                              | 54%                              | 65%   | 84%   | 26%   |

Table 1: Numerical comparison of  $|B_1^+|$  and  $|B_1^-|$ . The average over central axial slice was calculated within a circular region of interest with 25cm radius.